AJNR

This information is current as of April 18, 2024.

Diffusion-weighted Imaging Patterns of Brain Damage Associated with Cerebral Venous Thrombosis

Denis Ducreux, Catherine Oppenheim, Xavier Vandamme, Didier Dormont, Yves Samson, Gérald Rancurel, Guy Cosnard and Claude Marsault

Diffusion-weighted Imaging Patterns of Brain Damage Associated with Cerebral Venous Thrombosis

Denis Ducreux, Catherine Oppenheim, Xavier Vandamme, Didier Dormont, Yves Samson, Gérald Rancurel, Guy Cosnard, and Claude Marsault

BACKGROUND AND PURPOSE: **Apart from cases studies, little is known regarding diffusion-weighted imaging of brain lesions associated with human cerebral venous thrombosis (CVT). Our aim was to describe the initial diffusion-weighted imaging patterns observed in brain areas with MR signal changes associated with CVT and to compare them with those of follow-up imaging.**

METHODS: **The cases of nine patients with brain lesions associated with CVT who underwent CT and diffusion-weighted imaging 3 hours to 4 days after sudden neurologic onset were retrospectively reviewed. The apparent diffusion coefficient (ADC) in abnormal brain was compared with that of contralateral normal regions using z score analysis. MR images obtained during 3 to 6 months of follow-up were available for seven patients.**

RESULTS: **All patients had nonhemorrhagic T2-hyperintense brain regions. These were associated with partially hemorrhagic areas on the CT scans of four patients. In nonhemorrhagic edematous areas, ADC was heterogeneous (coexistence of increased, normal, or decreased ADC) in five patients and homogeneous in four. In the latter four patients, ADC values were within normal range in three, whereas a large homogeneous hyperintensity with decreased ADC values $(0.3–0.4\ 10^{-3}mm^2/s, < -3\ z$ scores) was observed in one. When available, follow-up images always showed hemorrhagic sequelae in initially hemorrhagic areas. Nonhemorrhagic edematous areas with initially increased ADC values returned to normal. Initially normal or decreased ADC values were predictive of reversibility, although imaging sequelae were rarely observed.**

CONCLUSION: **The diffusion-weighted imaging/ADC pattern of venous stroke is more heterogeneous than previously thought. Large brain regions of reduced ADC values that are not predictive of ultimate infarction in cases of CVT can be observed.**

Diffusion-weighted MR imaging is increasingly used for diagnostic purposes in cases of acute stroke (1–3). In contrast to the documented diagnostic power of diffusion-weighted imaging for acute arterial stroke, little is known regarding the diffusion-weighted imaging pattern of venous stroke. In a previous experimental report (4) and in human case studies (5–7) of diffusion-weighted imaging in cases of cerebral venous thrombosis (CVT), the apparent diffusion coefficient (ADC)

was shown to be decreased (4–6), normal (6), or increased (7). Moreover, the prognostic value of the ADC in acute venous stroke is still debated, although it has been recently suggested that diffusion-weighted imaging could noninvasively help in selecting those patients with CVT who would benefit from more aggressive treatments (5). Our aim was to describe the initial diffusion-weighted brain imaging/ADC patterns associated with CVT, to determine whether these patterns differ from the known diffusion-weighted imaging patterns of arterial stroke, and to evaluate the predictive value of initial diffusion-weighted imaging/ADC on imaging sequelae of the brain after CVT.

Methods

Patients

From a database of 30 patients with a proven diagnosis of CVT, who underwent MR imaging between December 1997 and February 2000, we retrospectively selected those who had experienced a sudden onset of acute neurologic symptoms and

who had undergone unenhanced CT and MR imaging, including diffusion-weighted imaging performed within 4 days of neurologic onset. Nine patients (all women; age range, 20–65 years; mean age, 40.1 years) fulfilled these criteria. Before undergoing imaging, all patients complained of progressive headaches and underwent emergent clinical evaluation by a stroke neurologist because of sudden neurologic symptoms: sensorimotor deficit (n = 8), aphasia (n = 2), loss of cognitive functions (n = 1), and seizures (n = 3). Delay from the time of sudden onset of these neurologic symptoms to initial MR imaging ranged from 3 hr to 4 days (1.6 ± 1.4 [mean ± SD] days). The diagnosis of CVT was assessed by only MR angiography in five cases, by MR angiography and angio-CT in two cases, and by digital angiography and MR angiography in the other two cases. CVT exclusively involved the superficial venous system (cortical veins, superior sagittal sinus, and transverse sinuses) in seven patients and the superficial and the deep venous system (vein of Galen, straight sinus or internal cerebral veins) in two patients. Associated conditions were found in all except one patient: nicotinism and contraceptive therapy (n = 4), polycythemia vera (n = 1), anemia (n = 2), and sinusitis (n = 1). For all patients, heparin therapy was initiated immediately after the positive diagnosis of CVT. In addition, two patients were treated by in situ thrombolysis. The demographic and clinical data of the nine studied patients are presented in the Table.

Initial MR Imaging

Four MR imaging sequences were performed with a 1.5-T MR unit. For the T1-weighted sequence, the parameters were as follows: imaging time, 3 min; sagittal or axial interleaved sections, 5 mm; matrix, 512 × 224; field of view, 24 × 24 cm; 425/20 (TR/TE); and bandwidth, 32 kHz. For the fast fluid-attenuated inversion recovery (FLAIR) imaging sequence, the parameters were as follows, imaging time, 4 min; axial interleaved sections, 5 mm; matrix, 256 × 256; field of view, 24 × 24 cm; 10002/148/2200 (TR/TE$_{eff}$/TI); and bandwidth, 32 kHz. For the 2D time-of-flight imaging sequence, the parameters were as follows: interleaved sections, 90 × 2 mm; matrix, 256 × 256; field of view, 22 × 22 cm; 20/6.5 (TR/TE); flip angle, 60 degrees; bandwidth, 15.63 kHz; and coronal sections were obtained for all patients, except one patient with a deep CVT. For two patients, prototype diffusion-weighted imaging sequences were obtained with the following parameters: imaging time, 1 min; images, multisection single shot spin-echo diffusion echo-planar with a pair of diffusion gradients centered around the 180-degree pulse; axial section thickness, 6 mm; section gap, 1.5 mm; matrix, 96 × 64; field of view, 28 × 21 cm; 4000/120 (TR/TE$_{eff}$); and five sets of 17 sections were acquired with five b values (duration = 25 ms, separation time = 28 ms), starting from baseline echo-planar imaging T2 (b = 0 s/mm²) up to 800 s/mm² with diffusion gradients applied in three orthogonal spatial directions. For the other seven patients, modified diffusion-weighted imaging sequences were obtained with the following parameters: imaging time, 11 s; images, multisection single-shot spin-echo echo-planar with a pair of diffusion gradients centered around the 180-degree pulse; axial section thickness, 6 mm; section gap, 1.5 mm; 2825/92.6 (TR/TE$_{eff}$), matrix, 96 × 64; field of view, 28 × 21 cm; and 16 sections were acquired with echo-planar imaging T2 acquisition (b = 0 s/mm²) and a b = 1000 s/mm² (diffusion gradient G = 22mT/m, duration = 32 ms, separation time = 39 ms). The diffusion gradients were successively and separately set in the three orthogonal directions, and isotropic images were generated.

Image Analysis

To acquire ADC calculations, one neuroradiologist visually selected all brain areas with signal changes on diffusion-weighted and/or T2-weighted echo-planar images (ie, b = 0 s/

mm²) for each patient. A dedicated software tool (FuncTool) was used to generate quantitative ADC maps. Small circular regions of interest (ROI) of 45 mm² (16 pixels) were centered around areas with abnormal signal on the diffusion-weighted or T2-weighted images to calculate mean ADC values. According to the extent and the signal heterogeneity of the lesion, two to seven ROI per patient were positioned in the brain area with MR signal changes. Mirror ROI were positioned symmetrically in the contralateral areas, which appeared normal on both diffusion-weighted and FLAIR images. Overall, 37 × 2 measurements were obtained in abnormal and normal-appearing brain regions. Mirror ADC measurements were then averaged to obtain a reference normal ADC value (0.88 ± 0.15 10⁻³ mm²/s). Mean ADC values measured in each ROI positioned in the stroke lesion were compared with the normal ADC value using a z score analysis. Increased and decreased ADC values were those with z scores >2 and <−2, respectively.

To assess hemorrhage, unenhanced CT scans and T1-weighted MR images were reformatted in the same plane as that of the initial diffusion-weighted images, using a dedicated software tool (VoxTool). For each ROI positioned in the lesion shown on a diffusion-weighted image, we looked for the presence of hyperdensity on the corresponding CT scan and/or hyperintensity on the T1-weighted images. ROI were considered hemorrhagic whenever a hyperdense area was present on the unenhanced CT scan or if a hyperintensity was observed on the T1-weighted images.

A follow-up study indicated that one patient had died within 1 week of the onset of symptoms and that one patient was lost to follow-up. The other seven patients underwent clinical and MR imaging follow-up for 3 to 6 months after the onset of symptoms. For one patient (patient 3) who was unable to lie still in the scanner, image quality was insufficient to assess sequelae in part of the lesion precisely. Overall, follow-up MR images were available of 26 of the 37 ROI positioned within the stroke lesion. The follow-up MR images were reformatted in the same plane as that of the initial diffusion-weighted images by use of a dedicated software tool (VoxTool). For each ROI initially positioned in the lesion shown on a diffusion-weighted image, two neuroradiologists independently qualitatively assessed for the presence of brain atrophy or hemorrhagic sequelae in the corresponding area on the follow-up MR images. The final result was reached by consensus.

Results

Venous lesions were all supratentorial. In seven patients, lesions were located predominantly in the cortical-subcortical area, and in two patients, lesions involved the gray nuclei and the subcortical areas. The venous lesions were iso- or hypointense on T1-weighted sequences and hypo-, iso-, or hyperintense on T2-weighted sequences. On diffusion-weighted images, hyperintensity covered the whole stroke lesion for six patients. In contrast, mixed hypo-/hyperintense areas were observed on the diffusion-weighted images of three patients. ADC values were all significantly decreased for one patient with a deep CVT (patient 9) (Fig 1) and were within the normal range for three patients (patients 6, 7, and 8). For three other patients (patients 1, 2, and 4), increased ADC values were associated with normal ADC values (Fig 2). For the remaining two patients (patients 3 and 5), increased, decreased, and normal ADC values were observed in different ROI (Fig 3).
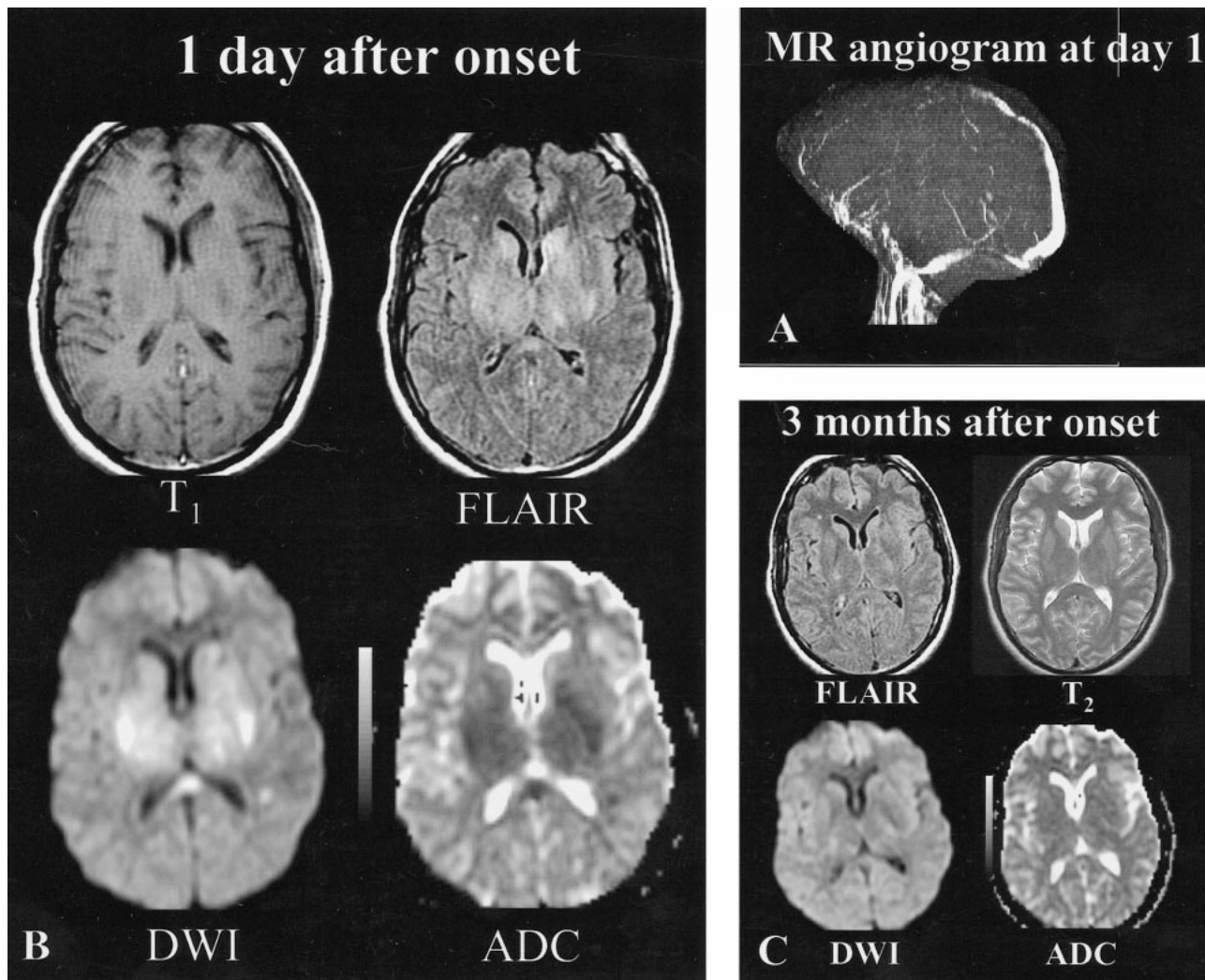
FIG 1.   Patient 9, a 34-year-old woman with headaches, cognitive function loss, and sudden-onset right hemiparesis.

A, MR angiogram (axial 2D time-of-flight method, maximum intensity pixel reconstruction, lateral view), obtained 1 day after the onset of neurologic symptoms, shows an occlusion of the deep and superficial venous systems (vein of Galen, straight sinus, internal cerebral veins, anterior part of the superior sagittal sinus).

B, Initial MR image obtained 1 day after the onset of neurologic symptoms. Axial spin-echo T1-weighted image shows bilateral areas of hypointensity at the level of the capsulae. Initial fast-FLAIR (10002/148/2200 [TR/TE/TI]) and diffusion-weighted (4000/120 [TR/TE], b = 1000 s/mm^2) images show widespread bilateral areas of hyperintensity in putamen, caudate nuclei, and the capsulae. ADC maps show markedly decreased ADC values (0.33–0.42 10^{-3} mm^2/s) (ie, *z* scores <-3 when compared with normal-appearing brain).

C, Follow-up MR image obtained 3 months after onset shows normal-appearing brain at the level of the gray nuclei, indicating that most lesions with initially decreased ADC values were reversible. Only focal slight areas of hyperintensity were visible in the centrum semiovale (not shown). Symptoms regressed completely within a few weeks.

Nonhemorrhagic areas were observed in all patients but coexisted with hemorrhagic areas in four patients. In the non-hemorrhagic areas, decreased ADC values (range, 0.33–0.58 10^{-3} mm^2/s; *z* score, -3.67 to -2.01) were found in three patients (patients 3, 5, and 9) (Fig 1). Four patients (patients 1, 2, 3, and 4) had areas of significantly increased ADC values (range, 1.21–1.74 10^{-3} mm^2/s; *z* score, 2.20–5.73). Other ADC values were within the normal range (range, 0.59–1.13 10^{-3} mm^2/s; *z* score, -1.91 to 1.67).

The clinical and imaging follow-up data are presented in the Table. No discrepancies existed between the assessments made of imaging sequelae by the two neuroradiologists. Of the seven patients

with follow-up images, six were free of clinical sequelae. In initially hemorrhagic areas, hemorrhagic sequelae were seen on the follow-up MR images of all patients (Fig 2). In nonhemorrhagic areas, initially normal or increased ADC values were normal on the follow-up MR images (patients 2, 3, 4, 6, and 8). One patient (patient 5) had focal atrophy revealed by the follow-up MR images (Fig 3). In the latter patient, although ADC values were considered normal in part of the nonhemorrhagic area, they were at the lower limit of normal values (*z* score = -1.91). In nonhemorrhagic areas with initially decreased ADC values, sequelae were also observed in this patient (patient 5). Conversely, the large area with an initially homogeneous decrease
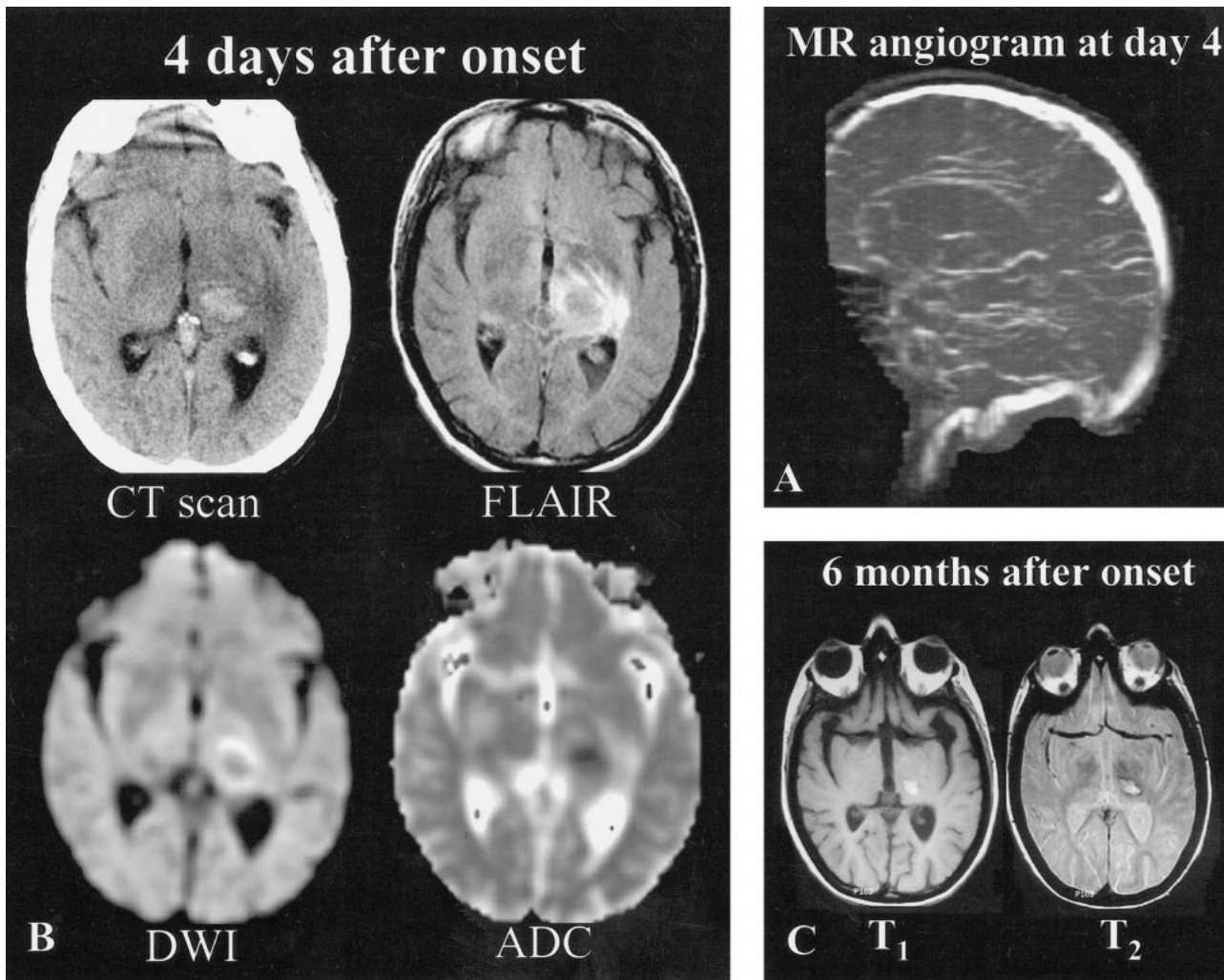
FIG 2.   Patient 2, a 41-year-old woman with vomiting, headaches, right hemianopsia, and right sensorimotor deficit of sudden onset.

A, MR angiogram (coronal 2D time-of-flight method, maximum intensity pixel reconstruction, lateral view), obtained 4 days after the onset of neurologic symptoms, shows an occlusion of the deep venous system (internal cerebral veins, straight sinus, vein of Galen). The right transverse sinus was also occluded (not shown).

B, Initial MR imaging and CT were performed 4 days after the onset of neurologic symptoms. CT scan shows a left capsulothalamic hematoma surrounded by edema. Axial FLAIR (10002/148/2200 [TR/TE/TI]) and diffusion-weighted (4000/120 [TR/TE], b = 1000 s/mm^2) images show central thalamic hypoisointensity surrounded by areas of hyperintensity. ADC values (0.59 10^{-3} mm^2/s) measured in the hemorrhagic thalamic lesion are at the lower limit of the normal range (z score of -1.91) and increased at the periphery (1.3 10^{-3} mm^2/s, z score = 2.8).

C, Three months later, right hemiparesis persists along with areas of hyperintensity on T1- and T2-weighted images, suggesting the presence of hemorrhagic sequelae.

in ADC values seen on the image of another patient (patient 9) almost completely resolved, with only small foci of hyperintensity in the centrum semiovale visible on the 3-month follow-up MR image (Fig 1).

Discussion

Diffusion-weighted imaging is a technique in which images display local movement possibilities of water molecules (2, 3), and it has been extensively used in cases of acute arterial stroke. Water shifts from the extracellular to the intracellular compartment (ie, cytotoxic edema) that occur at the early stage of arterial stroke are thought to be responsible for the hyperintensity on diffusion-weighted images and for the drop in ADC values (1). Thus, diffusion-weighted imaging potentially distinguishes between cytotoxic and vasogenic edema (8). Experimental results (9, 10) suggest that decreased ADC values reflect cellular edema and that increased ADC values correspond to an increase in the extracellular space (ie, vasogenic edema) (11, 12).

The pathophysiology of venous stroke remains obscure. Venous flow obstruction is thought to result in raised intracranial pressure (13), decreased cerebral blood flow (14), and reduced cerebral perfusion pressure (4), subsequently leading to venous infarction (15). As a result of venous congestion and disruption of the blood-brain barrier, the net capillary filtration increases, leading to progressive
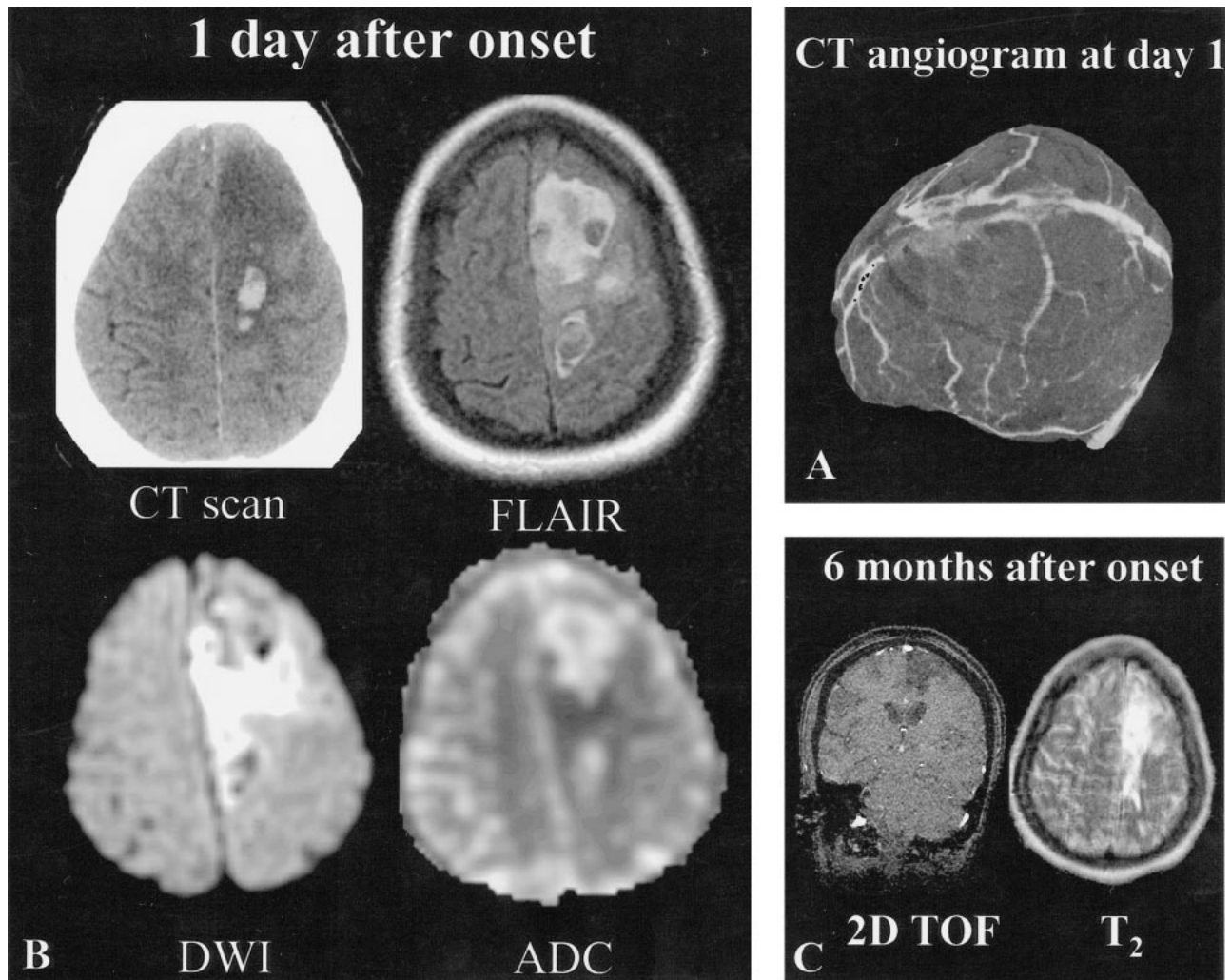
FIG 3. Patient 5, a 20-year-old woman with seizures and left motor deficit of sudden onset.

A, CT angiogram, obtained 1 day after onset, shows an occluded superior sagittal sinus. The deep venous system was intact (not shown).

B, Initial MR imaging and CT were performed 1 day after onset. CT scan shows a large area of hypodensity with focal areas of hyperdensity corresponding to a recent hematoma. Axial FLAIR (10002/148/2200 [TR/TE/TI]) and diffusion-weighted (4000/120 [TR/TE], b = 1000 s/mm²) images show a heterogeneous area with predominant areas of hyperintensity and hypointensity at the site of the hematoma seen on the CT scan. ADC map shows mixed areas of increased ADC values (1.66 10^{-3} mm²/s) (ie, *z* score >3), at the lower limit of normal values (0.59 10^{-3} mm²/s) (ie, *z* score = −1.9), or slightly decreased ADC values (0.58 10^{-3} mm²/s) (ie, *z* score <−2).

C, Follow-up MR image obtained 6 months after onset shows left frontal sequelae in areas with initially decreased or normal ADC values (2D time-of-flight source image used to illustrate MR sequelae). The patient had no clinical deficit.

cerebral edema (16). Vasogenic edema was initially considered to be the type of edema predominating in venous stroke (4). This was recently reinforced by the diffusion-weighted imaging findings of a patient with venous stroke who underwent imaging 1 day after the onset of acute neurologic symptoms; in the acute phase, ADC values were increased, suggesting that vasogenic edema was predominant (7). In our study, we also found large areas of increased ADC values in five of the nine studied patients who underwent imaging within 4 days of the onset of symptoms. As previously reported (7, 8), this indicates impaired but viable tissue, because these areas with initially increased ADC were free of sequelae on the follow-up MR images.

It has recently been proposed that cytotoxic edema contributes to the cascade of pathologic events in experimental (4, 13) and human (5) venous stroke. A diffusion-weighted imaging study of CVT in rats showed a 56% decline in ADC values 30 min after experimental CVT was induced (4). In line with these experimental results, we observed decreased ADC values in three patients with acute venous stroke. In one of them, we observed large areas of decreased ADC values that were within the range of ADC values usually reported in association with pure acute arterial stroke (1, 3); however, differences exist between arterial and venous stroke. Previous studies of CVT have shown cerebral blood flow reductions well below the

Synopsis of clinical and imaging findings and follow-up in nine patients with venous stroke

Patient	Age (yrs)/ Sex	Delay to MR Imaging	Symptoms and Clinical Course	Associated Conditions	Infarct Location	CVT Location	Therapy	Clinical Outcome	MR Sequelae
1	32/F	1 day	Progressive headaches and confusion; visual hallucinations, focal motor deficit of right superior arm of sudden onset	Seizures, mental deficiency	Left temporal and occipital lobes; left corona radiata	Superior sagittal sinus and left transverse sinus	Heparin therapy; in situ thrombolysis with thromboaspiration	Died 8 days after admission	Not available
2	41/F	4 days	Vomiting, headaches; right superior and inferior limb sensorimotor deficit, right hemianopsia	Contraceptive therapy	Left thalamus and capsulae; left temporal lobe	Right transverse sinus, temporal vein and vein of Galen	Heparin therapy; in situ thrombolysis 5 days after neurologic deficit	Right hemiparesis	Left thalamus
3	37/F	4 days	Left hand sensorimotor deficit, right temporal headaches	Nicotinism and contraceptive therapy	Right frontal and parietal lobes; right centrum semiovale	Right transverse sinus	Non-steroid antiinflammatory and antiepileptic	Free of symptoms	None
4	65/F	3 hours	Vomiting and headaches for 15 days; right superior arm motor deficit, aphasia of sudden onset, with seizures	Anemia (gastric ulcer)	Left frontal and parietal lobes	Superior sagittal sinus, right and left transverse sinuses	Heparin therapy and antiepilectic	Free of symptoms	None
5	20/F	1 day	Seizures, headaches; left superior or arm motor deficit	Caeliac disease with anemia	Left frontal lobe	Superior sagittal sinus	Heparin therapy	Free of symptoms	Left frontal lobe
6	57/F	1 day	Left headaches, aphasia and memory loss dysfunction	Nicotinism and contraceptive therapy	Left temporal lobe	Left transverse sinus	Heparin therapy	Free of symptoms	None
7	55/F	1 day	Headaches; right facial motor deficit	Polycythemia vera	Left temporal lobe	Left transverse sinus	Heparin therapy	Lost to follow-up	Not available
8	20/F	1 day	Headaches, seizures; left superior or arm motor deficit	Contraceptive therapy	Right parietal lobe	Superior sagittal sinus	Heparin therapy	Free of symptoms	None
9	34/F	1 day	Progressive headaches; cognitive functions loss, right motor deficit	Sinusitis	Right and left corona radiata; right putamen	Vein of Galen, straight sinus, internal cerebral veins, and superior sagittal sinus	Heparin therapy	Free of symptoms	None

threshold for cytotoxic edema formation (17, 18). In the event of severe blood flow reduction in arterial thrombosis, the tissue is rapidly and irreversibly damaged, resulting in ischemic cell necrosis. In venous thrombosis, perfusion of the affected brain tissue might still be possible at lower flow rates, if the blood is drained through collateral pathways (13). With such flow conditions, however, swollen cells might be functionally but not irreversibly damaged and therefore have a potential for recovery (19, 20). Thus, decreased ADC in abnormal brain areas associated with CVT might not have the same prognostic value as those associated with pure arterial stroke. As shown in this study, brain areas with strongly decreased ADC values can return to normal in cases of CVT. Conversely, in a recent case study of human CVT, Manzione et al (5) suggested that quantitative diffusion-weighted imaging could be useful for establishing a threshold for permanent neurologic injury and thus help in selecting those patients who will benefit from more aggressive management. Although it is tempting to draw an analogy with arterial stroke, the heterogeneous ADC pattern we observed in most cases and the fact that ADC measurements fail to predict sequelae on follow-up MR images in some cases suggest that caution is needed in interpreting diffusion-weighted imaging/ADC changes in brain lesions associated with CVT. Two poorly controlled parameters can hinder ADC interpretation in cases of CVT: hemorrhagic transformation in venous stroke and the time point for brain damage.

Hemorrhagic areas were initially observed on the CT scans of four patients. The ADC values in hemorrhagic areas have not been reported in this small sample of patients because the susceptibility effects due to blood products can hinder ADC calculations. Because of the signal loss induced by blood products on strongly susceptibility-weighted MR sequences, such as echo-planar diffusion-weighted imaging, ADC software may fail to compute ADC values in hemorrhagic areas properly. In this study, we distinguished hemorrhagic area as proven by CT scan from nonhemorrhagic area. This dichotomy is somewhat arbitrary because CT and spin-echo sequences are not optimal for the detection of acute petechial hemorrhage. A T2-weighted gradient-echo sequence was not part of our imaging protocol but might well have displayed numerous petechial hemorrhages in the areas that we considered to be nonhemorrhagic.

The time at which brain damage occurred is the second parameter that is crucial when interpreting ADC changes. Unfortunately, the precise time point of CVT is often unknown because the course of the disease in humans can proceed over days and weeks (4, 20, 21); however, all the patients in our study experienced sudden onset of neurologic symptoms, which most likely provides an approximate indication of the onset of tissue infarction and the occurrence of edema. The time point of venous stroke is more precisely known in experimental models of CVT (4). Cytotoxic edema has been shown to be rapidly followed by vasogenic edema, as witnessed by ADC values returning almost to normal within 48 hr in animal models (4). Considering the uncertainty regarding the time point of brain damage in human CVT, the simultaneous presence of both of these edematous components is likely and might result in apparently normal ADC values, similar to those observed in all except one of our patients.

Our method of ADC calculation has some pitfalls: we used relatively small ROI to avoid partial volume effect on ADC values; however, ADC values calculated on a pixel-by-pixel basis were averaged over ROI of 45 mm². This would mask local ADC changes because ROI containing the same amount of pixels of low and high ADC values would result in normal averaged ADC. In addition, we used ADC in the contralateral normal-appearing brain matter as a reference for normal ADC values. Consequently, ADC values measured in cortical, subcortical, and white matter were pooled to obtain normal ADC values. Ideally, ADC in abnormal gray or white matter should be compared with that of normal gray or white matter, respectively. When positioning an ROI in a heterogeneous venous stroke lesion, it is often impossible to distinguish between cortical, subcortical, and white matter.

Conclusion

Several conclusions can be drawn from our results. The diffusion-weighted imaging/ADC pattern of brain lesions associated with CVT is more heterogeneous than initially thought. Although in most patients, this pattern differs markedly from that of pure arterial stroke, extended homogeneous areas of decreased ADC can be observed in the images of recent brain lesions associated with CVT. In terms of prognosis, nonhemorrhagic areas with initially increased or normal ADC have a good prognosis and areas with initially decreased ADC values can also be reversible.

References

1. Warach S, Gaa J, Siewert B, Wielopolski P, Edelman RR. **Acute human stroke studied by whole brain echo planar diffusion-weighted magnetic resonance imaging.** *Ann Neurol* 1995;37: 231–241
2. Le Bihan D, Breton E, Lallemand D, Grenier P, Cabanis E, Laval-Jeantet M. **MR imaging of intravoxel incoherent motions: application to diffusion and perfusion in neurologic disorders.** *Radiology* 1986;161:401–407
3. Moseley ME, Cohen Y, Mintorovitch J, et al. **Early detection of regional cerebral ischemia in cats: comparison of diffusion- and T2-weighted MRI and spectroscopy.** *Magn Reson Med* 1990;14:330–346
4. Rother J, Waggie K, van Bruggen N, de Crespigny AJ, Moseley ME. **Experimental cerebral venous thrombosis: evaluation using magnetic resonance imaging.** *J Cereb Blood Flow Metab* 1996;16:1353–1361
5. Manzione J, Newman GC, Shapiro A, Santo-Ocampo R. **Diffusion- and perfusion-weighted MR imaging of dural sinus thrombosis.** *AJNR Am J Neuroradiol* 2000;21:68–73

6. Corvol JC, Oppenheim C, Manai R, et al. **Diffusion-weighted magnetic resonance imaging in a case of cerebral venous thrombosis.** *Stroke* 1998;29:2649–2652

7. Keller E, Flacke S, Urbach H, Schild HH. **Diffusion- and perfusion-weighted magnetic resonance imaging in deep cerebral venous thrombosis.** *Stroke* 1999;30:1144–1150

8. Schaefer PW, Buonanno FS, Gonzalez RG, Schwamm LH. **Diffusion-weighted imaging discriminates between cytotoxic and vasogenic edema in a patient with eclampsia.** *Stroke* 1997;28:1082–1085

9. Ito J, Marmarou A, Barzo P, Fatouros P, Corwin F. **Characterization of edema by diffusion-weighted imaging in experimental traumatic brain injury.** *J Neurosurg* 1996;84:97–103

10. Loubinoux I, Volk A, Borredon J, et al. **Spreading of vasogenic edema and cytotoxic edema assessed by quantitative diffusion and T2 magnetic resonance imaging.** *Stroke* 1997;28:419–426

11. Kuroiwa T, Nagaoka T, Ueki M, Yamada I, Miyasaka N, Akimoto H. **Different apparent diffusion coefficient: water content correlations of gray and white matter during early ischemia.** *Stroke* 1998;29:859–865

12. Ito J, Marmarou A, Barzo P, Fatouros P, Corwin F. **Characterization of edema by diffusion-weighted imaging in experimental traumatic brain injury.** *J Neurosurg* 1996;84:97–103

13. Frerichs KU, Deckert M, Kempski O, Schurer L, Einhaupl K, Baethmann A. **Cerebral sinus and venous thrombosis in rats induces long-term deficits in brain function and morphology:** evidence for a cytotoxic genesis. *J Cereb Blood Flow Metab* 1994;14:289–300

14. Kanaiwa H, Kuchiwaki H, Inao S, Sugita K. **Changes in the cerebrocortical capillary network following venous sinus occlusion in cats.** *Surg Neurol* 1995;44:172–181

15. Nakase H, Kakizaki T, Miyamoto K, Hiramatsu K, Sakaki T. **Use of local cerebral blood flow monitoring to predict brain damage after disturbance to the venous circulation: cortical vein occlusion model by photochemical dye.** *Neurosurgery* 1995;37:280–285

16. Ito K, Tsugane R, Ikeda A, Suzuki Y, Sato K. **Cerebral hemodynamics and histological changes following acute cerebral venous occlusion in cats.** *Tokai J Exp Clin Med* 1997;22:83–93

17. Kurokawa Y, Hashi K, Okuyama T, Uede T. **Regional ischemia in cerebral venous hypertension due to embolic occlusion of superior sagittal sinus in rat.** *Surg Neurol* 1990;34:390–395

18. Gotoh M, Ohmoto T, Kuyama H. **Experimental study of venous circulatory disturbance by dural sinus occlusion.** *Acta Neurochir (Wien)* 1993;124:120–126

19. Nakase H, Nagata K, Otsuka H, Sakaki T, Kempski O. **Local cerebral blood flow autoregulation following "asymptomatic" cerebral venous occlusion in the rat.** *J Neurosurg* 1998;89:118–124

20. Preter M, Tzourio C, Ameri A, Bousser MG. **Long-term prognosis in cerebral venous thrombosis: follow-up of 77 patients.** *Stroke* 1996;27:243–249

21. Villringer A, Mehraein S, Einhäupl KM. **Pathophysiological aspects of cerebral sinus venous thrombosis (SVT).** *J Neuroradiol* 1994;21:72–80